

Chaotic Ionization of Nonhydrogenic Alkali Rydberg States

Andreas Krug^{1,2} and Andreas Buchleitner¹

¹Max-Planck-Institut für Physik komplexer Systeme, Nöthnitzer Strasse 38, D-01187 Dresden, Germany

²Max-Planck-Institut für Quantenoptik, Hans-Kopfermann-Strasse 1, D-85748 Garching, Germany

(Received 18 December 2000)

We report the first *ab initio* quantum treatment of microwave driven alkali Rydberg states. We find that nonhydrogenic atomic initial states exhibit fingerprints of classically chaotic excitation, and identify the cause of their experimentally observed enhanced ionization, as compared to Rydberg states of atomic hydrogen.

DOI: 10.1103/PhysRevLett.86.3538

PACS numbers: 05.45.Mt, 32.80.Rm, 72.15.Rn

Rydberg states of atomic hydrogen are the perfect quantum analog of classical planetary motion. They incarnate the correspondence principle via the equivalence of the classical principal action and the principal quantum number n_0 , as well as of the classical Kepler frequency and the local energy spacing in the Rydberg progression. Also under strong periodic driving do they exhibit the essential features of the underlying classical dynamics [1], which go chaotic as the driving field amplitude F is increased. However, classically chaotic motion is tantamount to the destruction of symmetries and, hence, of good quantum numbers in the quantum system, which prevents us from identifying a single quantum state with a single chaotic classical trajectory. Therefore, a large number of quantum states, i.e., a large spectral density is needed as a prerequisite for quantum dynamics to resolve the intricate phase space structures of classically chaotic dynamics [1]. Furthermore, the periodic driving induces multiphoton transitions of variable order between atomic bound and continuum states, which finally gives rise to the ionization of the atom [2]. Indeed, it is the resulting ionization yield which is typically used as the experimental probe of the chaotic bound state dynamics [3].

In laboratory experiments, it is state of the art to produce atomic Rydberg states with principal quantum numbers n_0 between 20 and 120 [3–5], and, hence, large spectral densities (scaling as n_0^5). However, for driving frequencies in the microwave regime which are near resonant with the transition $n_0 \approx 57 \rightarrow n_0 + 1$ [6], chaotic ionization is mediated by multiphoton transitions of the order $k = 1/2n_0^2\omega \geq 29$ (simply given by the ratio of the initial state ionization potential to the photon energy). An exact theoretical/numerical treatment of the corresponding quantum mechanical eigenvalue problem defined by the T -periodic Hamiltonian

$$H(t) = \frac{\vec{p}^2}{2} + V_{\text{atom}}(r) + \vec{r} \cdot \vec{F}(t), \quad r > 0, \quad (1)$$

$$\vec{F}(t + T) = \vec{F}(t), \quad T = \frac{2\pi}{\omega},$$

in dipole approximation and using atomic units, with ω and \vec{F} the driving field frequency and amplitude, remained

untractable so far, simply due to its dimension [2]. Furthermore, for reasons of experimental convenience, a considerable part of the experiments was performed using Rydberg states of alkali [4,5,7] rather than of hydrogen atoms [3,6], starting out from the hypothesis that the driven dynamics of the highly excited Rydberg electron should not undergo any relevant changes due to the presence of a multielectron core which modifies the potential $V_{\text{atom}}(r)$ only in the immediate vicinity of the nucleus. All available data prove, nonetheless, the opposite: nonhydrogenic alkali Rydberg states appear to ionize at considerably lower driving field amplitudes than Rydberg states of atomic hydrogen [3,5,7]. This assertion, however, is hitherto based on a somewhat questionable comparison of the available hydrogen and alkali data, since relevant experimental parameters such as the atom-field interaction time or the driving field frequency are typically different for different experiments. As the experimentally observed ionization yield was shown to be explicitly time dependent [5], and since the scale invariance of the classical dynamics of the periodically driven two-body Coulomb problem prevails—*a priori*—only in the driven hydrogen atom [3,8] (where it allows one to realize the same classical ionization scenario for different driving field frequencies ω), the experimentally observed enhanced ionization of nonhydrogenic states of alkali atoms remains a puzzle for more than a decade [3,5]. Only a (laboratory or numerical) experiment which allows for the exclusive change of the atomic species (from hydrogen to alkali), fixing *all* other experimental parameters, can settle this long-standing problem. Yet, while laboratory experiments on alkali atoms are easier performed than on atomic hydrogen, the converse is true for a theoretical/numerical treatment. The alkali ionization problem is complicated by the fact that it additionally involves quantum mechanical scattering of the Rydberg electron off the multielectron core [8,9], on top of the mere size of the eigenvalue problem defined by (1). Only with the advent of the most powerful supercomputers, which provide us with the means to treat the described atomic ionization process in its full complexity, without any essential approximations nor adjustable parameters, are we now able to tackle this challenging problem.

It is the purpose of this Letter to present results of the first numerical experiment on the microwave ionization of nonhydrogenic states of lithium. These are compared to laboratory results on atomic hydrogen, obtained under identical experimental conditions.

Combining group theoretical methods for the description of the atomic degrees of freedom (including the continuum), R -matrix theory to include the nonvanishing quantum defects induced by the multielectron core [8], the Floquet theorem (a generalized version of the Bloch theorem familiar from solid state physics) to account for the periodic driving, complex dilation to extract the energies and ionization rates of the atomic eigenstates in the field [2], and an intelligent, parallel implementation of the Lanczos algorithm with excellent scalability, we have been able to perform the numerical experiment on nonhydrogenic $\ell_0 = 0$ angular momentum Rydberg states of lithium, for a linearly polarized microwave field, i.e., $\vec{r} \cdot \vec{F}(t) = Fz \cos(\omega t)$ in (1). We precisely chose the experimental parameters employed in laboratory experiments on atomic hydrogen [6], with the *only exception* of a finite quantum defect of the $\ell = 0, 1, 2, 3$ angular momentum states, and a well-defined atomic initial state $|n_0, \ell_0 = m_0 = 0\rangle$, with m_0 the angular momentum projection along the fixed field polarization axis. Furthermore, we assumed a constant microwave amplitude F experienced by the atoms, thereby neglecting pulse-induced switching effects. These, however, are of minor importance in this kind of experiment [2,3]. To be specific, the parameters were the driving field frequency $\omega/2\pi = 36$ GHz, the atom-field interaction time $t = 327 \times 2\pi/\omega$, principal quantum numbers in the range $n_0 = 28, \dots, 80$, and lithium quantum defects $\delta_{\ell=0} = 0.39947$, $\delta_{\ell=1} = 0.04726$, $\delta_{\ell=2} = 0.00213$, and $\delta_{\ell=3} = -8 \times 10^{-5}$ [10]. Correspondingly, the order of the multiphoton process to ionize the atomic initial state extends from $k \geq 15$ (for $n_0 = 80$) to $k \geq 120$ (for $n_0 = 28$), where we account for the shift of the effective ionization threshold to a finite value of the principal quantum number, $n_c \approx 105$, due to the finite size of the basis used for our numerical computations [2]. Note that such a shift also occurs in the laboratory experiment, due to unavoidable stray fields [3].

All calculations were performed on the CRAY T3E Garching (for $n_0 \geq 40$), and on the HITACHI SR8000-F1 Munich (for $n_0 < 40$, $k > 50$)—the latter one occupies position 1 in the international ranking [11] of top-level parallel computing facilities in the academic realm. To obtain converged low- n_0 results, the availability of the HITACHI SR8000-F1 was absolutely crucial. As an example, the eigenvalue problem which describes the ionization of $|n_0 = 28, \ell_0 = m_0 = 0\rangle$, for a given F , is defined by a banded, complex symmetric matrix of dimension 1 000 000 and width 6000. Approximately 4000 eigenvalues and eigenvectors have to be generated to gain all relevant spectral information, for the final calculation of the ionization yield.

Figure 1 shows a comparison of our numerical experiment to laboratory data obtained in the Stony Brook group [3,6]. The plot uses “scaled variables” [1] F_0 and ω_0 , i.e., the driving amplitude F and the driving frequency ω are measured in units of the Coulomb force ($\sim n_0^{-4}$) and of the Kepler frequency ($\sim n_0^{-3}$) along the unperturbed classical two-body Coulomb trajectory. Plotted is the ionization threshold field $F_0(10\%)$, i.e., the field amplitude needed to induce an ionization probability of 10% at given interaction time t and frequency ω , for different principal quantum numbers n_0 [1–5]. In a classical description of the driven two-body Coulomb problem, F_0 and ω_0 completely determine the classical phase space structure, what allows for an immediate interpretation of the experimental hydrogen data in Fig. 1 in terms of the underlying classical dynamics [3]. Most prominently, the hydrogen ionization threshold decreases almost monotonously in the frequency windows (II) and (III), and exhibits local maxima around $\omega_0 \approx 1.0 \dots 1.3$ and $\omega_0 \approx 2.0 \dots 2.5$, on top of a global

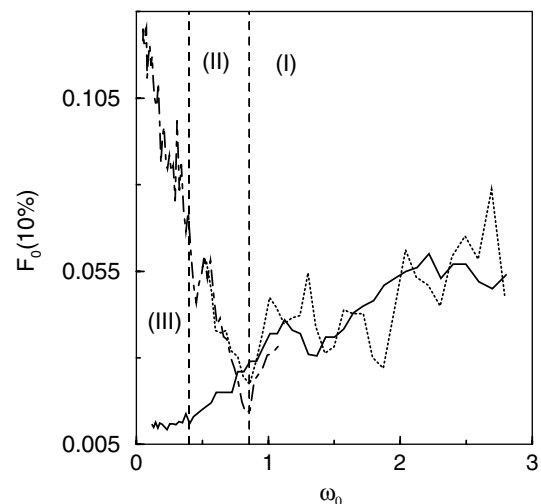


FIG. 1. Experimentally measured, scaled ionization threshold fields $F_0(10\%) = F(10\%)n_0^4$ of atomic hydrogen (dotted [6] and dash-dotted [3] curves), compared to our numerical experiment on the $|n_0, \ell_0 = m_0 = 0\rangle$ state of lithium (full curve), as a function of the scaled frequency $\omega_0 = \omega n_0^3$. The dotted curve was obtained under *precisely* the same conditions as the lithium data, i.e., at frequency $\omega/2\pi = 36$ GHz, interaction time $t = 327 \times 2\pi/\omega$, and principal quantum numbers within the range $n_0 = 28, \dots, 80$. Only ℓ_0 and m_0 were not well defined in the laboratory experiment, but microcanonically distributed over the energy shell [3,6]. Furthermore, the atoms experienced a finite rise and fall time of the microwave pulse in the laboratory (approximately 80 field cycles each [6]), whereas the numerical experiment assumes a constant value of F . These finite switching times of the microwave pulse are responsible for the more pronounced structures of the laboratory data as compared to the lithium results, but do not affect the globally very good agreement in the ω_0 interval (I). We also reproduce the experimental results obtained with $\omega/2\pi = 9.923$ GHz [3], to cover the low- ω_0 regime for hydrogen. (I), (II), and (III) distinguish scaled frequency ranges where $\omega > \Delta_{\text{hyd}}$, $\Delta_{\text{alk}} < \omega < \Delta_{\text{hyd}}$, and $\omega < \Delta_{\text{alk}}$, respectively; compare Fig. 2.

increase in the frequency window (I). The decrease in (III) and (II) essentially follows the classical ionization threshold which can be extracted, e.g., from classical 3D Monte Carlo simulations of the hydrogen experiments [3], whereas the global increase in (I) is a signature of dynamical localization [5,6], the analog of Anderson localization in the quantum transport of driven, chaotic, low-dimensional Hamiltonian systems [12]. The local maxima around $\omega_0 \approx 1.0$ and $\omega_0 \approx 2.0$ are a quantum signature of locally integrable [3] or “sticky” [13] classical dynamics, within or in the vicinity of nonlinear resonance islands in classical phase space.

Comparison of the laboratory to the numerical experiment immediately leads to the following observations:

(1) In the scaled frequency window (I), the ionization thresholds of nonhydrogenic Rydberg states of lithium follow the global trend of the hydrogen data, in particular, with the *same* absolute values of the driving field amplitude. Furthermore, the lithium data exhibit local maxima at $\omega_0 \approx 1.1$ and $\omega_0 \approx 2.2$, very much as the hydrogen data.

(2) There is a dramatic difference between hydrogen and lithium thresholds in the frequency window (II), where the lithium thresholds continue to increase with ω_0 , whereas the hydrogen thresholds decrease from rather high values, in accordance with classical results [1,3].

(3) The scaled lithium thresholds are essentially n_0 independent at very low values in the interval (III), whereas hydrogen exhibits (classical) thresholds approximately 10 to 20 times as large as for lithium, in this low-frequency regime.

The clue for understanding these features lies in the level structure of the unperturbed alkali spectrum which is illustrated in Fig. 2: For driving frequencies ω larger than or comparable to the energy difference $\Delta_{\text{hyd}}(n_0) \sim n_0^{-3}$ between neighboring hydrogen manifolds, and this is precisely in the regime (I), the driving field can efficiently mix hydrogenic and nonhydrogenic levels of the lithium atom, even for initial atomic states with nonvanishing quantum defect. Since in this frequency domain the essential symmetry properties of the driven two-body Coulomb problem below the ionization threshold prevail in the alkalis [8], also the transition to chaotic transport in the classical dynamics (i.e., the destruction of these symmetries) dominates the ω_0 or n_0 dependence of the ionization threshold of nonhydrogenic alkali Rydberg states, *despite* their manifestly nonclassical character due to the scattering of the Rydberg electron off the multielectron core [9].

For driving frequencies ω larger than the closest, energy gaining dipole transition frequency $\Delta_{\text{alk}}(n_0)$ starting out from the nonhydrogenic initial state, but smaller than $\Delta_{\text{hyd}}(n_0)$ [regime (II)], the driving field is still capable to efficiently couple different hydrogenic and nonhydrogenic states, whereas no comparable excitation mechanism is available in the hydrogen atom. Consequently, the general dependence of $F_0(10\%)$ on ω_0 is unaltered for lithium in this regime, whereas the hydrogen threshold is now deter-

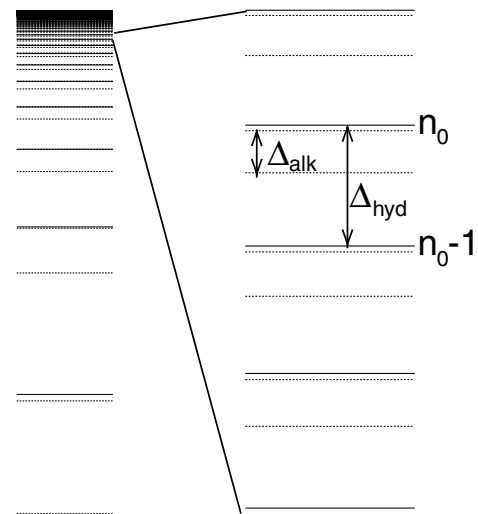


FIG. 2. Hydrogenic (full lines) and nonhydrogenic (dotted lines) energy levels of the unperturbed lithium atom, with a detail of the Rydberg progression on the right. In alkali atoms, the angular momentum degeneracy of the hydrogen spectrum is lifted by the multielectron core. The latter induces nonvanishing quantum defects δ_ℓ [10] of the low angular momentum states, which lead to the apparent energy shift of the nonhydrogenic with respect to the hydrogenic eigenstates. The relevant frequency scales for the ionization process, which define the intervals (I), (II), and (III) in Fig. 1 are $\Delta_{\text{hyd}}(n_0)$, the spacing of adjacent hydrogenic manifolds, and $\Delta_{\text{alk}}(n_0)$, the energy splitting corresponding to the first dipole-allowed upward transition leaving the nonhydrogenic initial state of the atom.

mined by the classical ionization process in the absence of near-resonant quantum mechanical transition amplitudes [1]. Accordingly, the alkali data display the general trend of increasing threshold with ω_0 , i.e., the signature of dynamical localization [6], over both frequency intervals (I) and (II), where only the former has a classical counterpart, not the latter. As a matter of fact, all currently available experimental data which exhibit dynamical localization in the ionization of nonhydrogenic alkali Rydberg [5,7] states have been obtained in regimes (II) and (III), which explains the apparent discrepancy (reaching a factor 10) between hydrogen and alkali thresholds to the largest extent. [A second, though secondary, reason is the systematically longer atom-field interaction times in the alkali as compared to the hydrogen experiments, which account for a correction of the observed threshold value which depends algebraically on t [5]. We can easily change the interaction time in our numerical experiment and verify that an increase of t by a factor 10 does not affect the qualitative difference observed in regime (II).]

Finally, at driving frequencies $\omega < \Delta_{\text{alk}}(n_0)$, even the alkali spectrum does not offer any atomic transition which allows for an efficient one-photon coupling of the initial atomic state to any other Rydberg level. This is clearly reflected by the transition from decreasing to essentially constant scaled threshold fields, which defines the borderline between (II) and the low-frequency range (III) in Fig. 1.

Only higher-order processes can induce efficient depletion of the initial state population, with subsequent ionization. The depletion rate of the nonhydrogenic initial state via a m -photon upward transition to the next Rydberg level can be estimated perturbatively, leading to a scaling of the threshold field as $F(10\%) \sim n_0^{-\alpha}$, where α grows from 4 to 4.6 for m increasing from 2 to 3. Such an estimation is consistent with our lithium data in Fig. 1, which cover the range from $n_0 = 39$ ($m = 2$) to $n_0 = 28$ ($m = 3$), in regime (III). However, it does not yet provide a very satisfactory picture of the ionization process in the low-frequency domain, since m is rapidly changing with n_0 , and no reliable estimation of the absolute value of $F(10\%)$ (depending on the coherent interplay of multiphoton transition amplitudes of different order connecting $|n_0\ell_0m_0\rangle$ to the continuum [14]) is included.

In summary, we performed an exact numerical experiment which allows — for the first time, in the experimentalist's as well as in the numerical laboratory — for the direct comparison of complex energy transport in Rydberg states of atomic hydrogen and of nonhydrogenic alkali atoms. Whereas laboratory experiments on atomic hydrogen and alkalis always differ by more than the finite quantum defects alone (interaction time, driving field frequency), the numerical experiment now allows for the appreciation of quantum scattering of the Rydberg electron off the multi-electron core, at otherwise *precisely identical* experimental conditions. Furthermore, our prediction of a marked transition from similar to distinct ionization dynamics of nonhydrogenic lithium Rydberg states as compared to atomic hydrogen can immediately be verified in the laboratory [4].

CPU time was provided by the Rechenzentrum Garching der Max-Planck-Gesellschaft, on a CRAY T3E, and by the Leibniz-Rechenzentrum der Bayerischen Akademie der Wissenschaften, München, on a Hitachi SR8000-F1.

-
- [1] G. Casati, B. V. Chirikov, D. L. Shepelyansky, and I. Guarneri, Phys. Rep. **154**, 77 (1987).
 - [2] A. Buchleitner, D. Delande, and J.-C. Gay, J. Opt. Soc. Am. B **12**, 505 (1995).
 - [3] P. M. Koch and K. A. H. Leeuwen, Phys. Rep. **255**, 289 (1995).
 - [4] M. W. Noel, W. M. Griffith, and T. F. Gallagher, Phys. Rev. A **62**, 063401 (2000).
 - [5] M. Arndt, A. Buchleitner, R. N. Mantegna, and H. Walther, Phys. Rev. Lett. **67**, 2435 (1991).
 - [6] E. J. Galvez, B. E. Sauer, L. Moorman, P. M. Koch, and D. Richards, Phys. Rev. Lett. **61**, 2011 (1988).
 - [7] Panming Fu, T. J. Scholz, J. M. Hettema, and T. F. Gallagher, Phys. Rev. Lett. **64**, 511 (1990).
 - [8] A. Krug and A. Buchleitner, Europhys. Lett. **49**, 176 (2000).
 - [9] T. Jonckheere, B. Grémaud, and D. Delande, Phys. Rev. Lett. **81**, 2442 (1998).
 - [10] C. J. Lorenzen and K. Niemax, Phys. Scr. **27**, 300 (1983).
 - [11] See <http://www.top500.org>
 - [12] S. Fishman, D. R. Grempel, and R. Prange, Phys. Rev. Lett. **49**, 509 (1982).
 - [13] J. G. Leopold and D. Richards, J. Phys. B **27**, 2169 (1994).
 - [14] A. Buchleitner, I. Guarneri, and J. Zakrzewski, Europhys. Lett. **44**, 162 (1998).